Journal of Inorganic and General Chemistry
ZAAC
Zeitschrift für anorganische und allgemeine Chemie
www.zaac.wiley-vch.de
RESEARCH ARTICLE
Check for updates
DOI: 10.1002/zaac.202200047

Cytotoxic Activities of Bis-cyclometalated Iridium(III) Complexes Containing Chloro-substituted κ^2N-terpyridines

Marion Graf,[a] Hans-Christian Böttcher,*[a] Peter Mayer,[a] Nils Metzler-Nolte,[b] Sugina Thavalingam,[b] and Rafał Czerwieniec[c]

Dedicated to Professor Wolfgang Beck on the Occasion of his 90th Birthday.

The synthesis and characterization of two new bis-cyclometalated compounds $[Ir(ptpy)_2(\kappa^2N\text{-terpy-}C_6H_4Cl\text{-}p)]PF_6$ [terpy-C_6H_4Cl-*p* = 4'-(4-chlorophenyl)-2,2':6',2''-terpyridine, (**1**)], and $[Ir(ptpy)_2(\kappa^2N\text{-terpy-Cl})]PF_6$ [terpy-Cl = 4'-chloro-2,2':6',2''-terpyridine, (**2**); ptpy = 2-(*p*-tolyl)pyridinato)] are described. The molecular structures of compounds **1** and **2** in the crystal were determined by single-crystal X-ray diffraction. **1** crystallized from dichloromethane/methanol/*iso*-hexane in the monoclinic space group $P2/_n$ and **2** from the same mixture of solvents in the triclinic space group P^-1. Photophysical investigations on **1** and **2** revealed broad unstructured luminescence in the red spectral region with the emission maxima in dichloromethane at 620 and 630 nm respectively. To explore cytotoxic properties of compounds **1** and **2**, a colorimetric assay (MTT assay) against prominent cancer cell lines, MCF-7 and HT-29, was performed. The determined IC_{50} values are in the low micromolar range (2–3 μM). In comparison to cisplatin, the tested complexes **1** and **2** exhibit up to > 20-fold (MCF-7) and > 40-fold (HT-29) increase in biological activity.

Introduction

Metal complexes have been widely studied for applications in the field of the development of new pharmaceutical metal-containing drugs.[1] In this light phosphorescent cyclometalated iridium(III) compounds belong to these compounds of potential candidates and play an important role in studies devoted towards therapy of cancers due to their high cytotoxic activities.[2] It could be shown that modifications of the cyclometalating as well as the ancillary ligands allowed a fine-tuning of the anticancer properties.[3] Moreover, interesting examples in using octahedral cyclometalated iridium(III) complexes were recently described to act as modulators in protein-protein interactions,[4] membrane disruptors,[5] mitochondria-targeted agents,[6] high-affinity sequence-selective DNA binders,[7] and even as receptor-targeted species.[8] Furthermore, these iridium(III) compounds have attracted increasing attention in bioimaging and biosensing applications.[9] Last but not least, very recently these compounds were studied in cancer treatment procedures using the photodynamic therapy (PDT) where they act as promising candidates of photosensitizers to support the generation of reactive oxygen species (ROS).[10]

In the course of related investigations we have a current interest in studies of the cytotoxic activity of bis-cyclometalated iridium(III) compounds towards some human cancer cell lines by examining the substituent influences in the sphere of the ancillary ligands.[11] Herein we describe the synthesis and the characterization of two new cyclometalated iridium(III) compounds of the type $[Ir(ptpy)_2(N\text{^}N)]PF_6$ [N^N = κ^2N-terpy-C_6H_4Cl-*p* = 4'-(4-chlorophenyl)-2,2':6',2''-terpyridine (**1**), and N^N = κ^2N-terpy-Cl = 4'-chloro-2,2':6',2''-terpyridine (**2**)]. Beside studies of the photophysical properties of **1** and **2**, which were supported by DFT and TD-DFT calculations, we demonstrated the potent in vitro antiproliferative activity of these new compounds.

Results and discussion

For the synthesis of the cationic mononuclear title complexes we used a bridge-splitting reaction starting from the dimeric precursor compound $[\{Ir(\mu\text{-Cl})(ptpy)_2\}_2]$ (ptpy = 2-*p*-tolylpyridinato) by the corresponding chelating terpy ligands in a dichloromethane/methanol/water mixture under reflux. The intermedi-

[a] M. Graf, H.-C. Böttcher, P. Mayer
Department Chemie
Ludwig-Maximilians-Universität
Butenandtstrasse 5–13 (D)
1377 München, Germany
Fax: +49-89-2180-77407
E-mail: hans.boettcher@cup.uni-muenchen.de
[b] N. Metzler-Nolte, S. Thavalingam
Faculty for Chemistry and Biochemistry
Chair of Inorganic Chemistry I – Bioinorganic Chemistry
Ruhr University Bochum
Universitätsstrasse 150
44801 Bochum, Germany
[c] R. Czerwieniec
Institute of Physical and Theoretical Chemistry
University Regensburg
Universitätsstrasse 31
3053 Regensburg, Germany

Supporting information for this article is available on the WWW under https://doi.org/10.1002/zaac.202200047

ate formed chloride salts $[Ir(ptpy)_2(N^N)]Cl$ yielded after metathesis with KPF_6 the corresponding hexafluoridophosphate derivatives (see Scheme 1).

Both new compounds were obtained as yellow-orange crystals and characterized by elemental analysis, ^1H and $^{13}C\{^1H\}$ NMR spectroscopy, mass spectrometry, and by UV-vis spectroscopy. Moreover, for **1** and **2** single-crystal X-ray diffraction

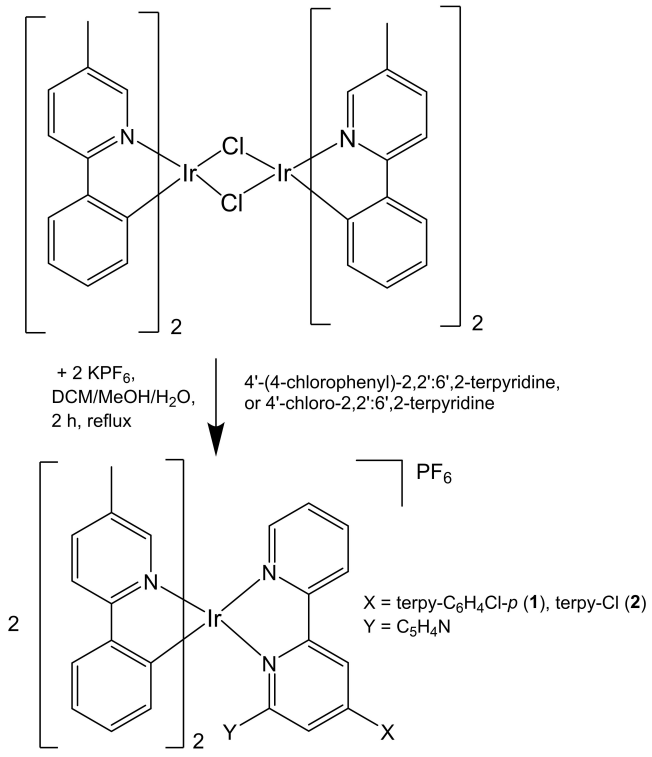

Scheme 1. Synthesis of compound **1** and **2**.

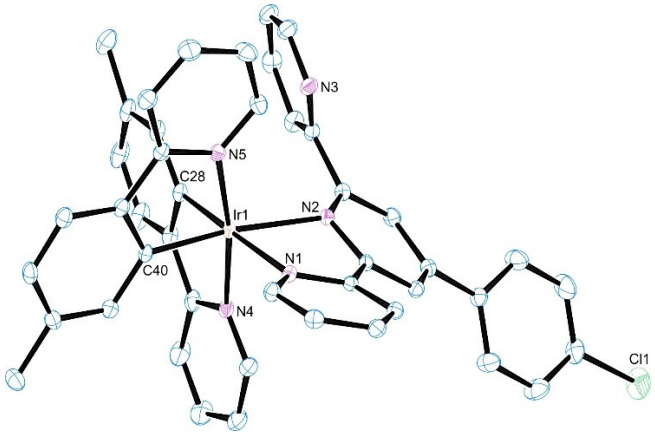

Figure 1. Molecular structure of the cation of **1** in the crystal (ORTEP drawing and atom labeling scheme with 50% probability level). Due to reasons of clarity all hydrogen atoms are omitted. Selected bond lengths/Å and angles/°: Ir1–N1, 2.127(3); Ir1–N2, 2.228(3); Ir1–N4, 2.053(3); Ir1–N5, 2.050(3); Ir1–C28, 2.018(3); Ir1–C40, 2.000(3). N1–Ir1–N2, 76.02(10); N4–Ir1–C28, 80.80(13); N5–Ir1–C40, 80.51(13).

studies were carried out. The ^1H and $^{13}C\{^1H\}$ NMR spectra of both new compounds confirmed the assumed molecular constitution. They illustrated the chemical inequivalence of the protons and the carbon atoms in the bisected backbone of the chloro-substituted terpyridine ligands caused by the κ^2N-coordination mode of the terpy ligand in each case. Moreover, two singlets in these spectra corresponding to different methyl groups hinted at the chemical non-equivalence of the two cyclometalated ligands in each case (see Experimental Section and Figures S1–S4 in the Supporting Information). Furthermore, the ESI mass spectra showed the molecular peaks for the mononuclear complexes.

Molecular Structure of Compounds 1 and 2

Compound **1** crystallized from a mixture of solvents containing dichloromethane/methanol/*iso*-hexane in the monoclinic space group $P2_1/n$ with four molecules in the asymmetric unit. A selected ORTEP view of the molecular structure of cations in **1** is shown in Figure 1. Selected bond lengths and angles are given in the caption.

The complex cation of **1** exhibits two cyclometalated 2-(*p*-tolyl)pyridinato ligands beside the substituted terpyridine ligand in a bidentate κ^2N-coordination mode. The three bidentate chelating ligands complete a distorted octahedral coordination sphere around the central iridium atom. The coordination sphere of the cation in **1** is best comparable with that of the known complex $[Ir(ppy)_2(\kappa^2N\text{-terpy-Cl})]^+$.[12] Thus, the three important bond angles in the central core of **1** (compare caption in Figure 1) agree very well with the reported corresponding ones for $[Ir(ppy)_2(\kappa^2N\text{-terpy-Cl})]^+$: N6–Ir2–N7, 76.40(15); N9–Ir2–C63, 80.19(16) and N10–Ir2–C74, 81.12(18).[12] The Ir–N and Ir–C bond parameters within the cyclometalated chelating ring systems were in good accordance with the usually observed ones in related compounds reported by us.[11] Compound **2** crystallized from a dichloromethane/methanol/*iso*-hexane mixture in the triclinic space group P^-1 with four molecules in the unit cell. An ORTEP view of the molecular structure of cations in **2** is shown in Figure 2. Selected bond lengths and angles are given in the caption.

The molecular structure of complex cations of **2** is closely related to those of compound **1** and, as mentioned before, best comparable with the complex $[Ir(ppy)_2(\kappa^2N\text{-terpy-Cl})]^+$.[12] Even in this case the important bond angles in the central distorted octahedral framework of the complex cation of **2** were found in a very good agreement with the observed ones in **1** and also in related literature compounds.[12]

Photophysical properties

Room temperature UV-vis absorption and emission of **1** and **2** were studied in dichloromethane solution. Respective spectra are shown in Figure 3 and pertinent data are listed in Table 1. The absorption spectra reveal strong features in the UV region and significantly weaker absorptions at longer wavelengths at

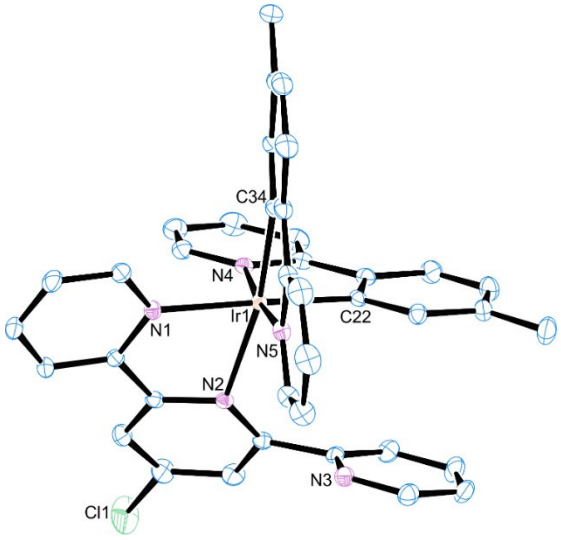

Figure 2. Molecular structure of the cation of **2** in the crystal (ORTEP drawing and atom labeling scheme with 50% probability level). Due to reasons of clarity all hydrogen atoms are omitted. Selected bond lengths/Å and angles/°: Ir1–N1, 2.138(3); Ir1–N2, 2.231(3); Ir1–N4, 2.053(3); Ir1–N5, 2.050(3); Ir1–C22, 2.016(3); Ir1–C34, 1.999(3). N1–Ir1–N2, 75.68(10); N4–Ir1–C22, 80.30(12); N5–Ir1–C34, 80.28(13).

Table 1. UV-vis absorption and luminescence data for **1** and **2** measured in dichloromethane at ambient temperature.

Compound	Absorption wavelength/nm (ε/$M^{-1}cm^{-1}$)[a]	Emission maximum/nm	Emission quantum yield[b]	Emission decay time/ns
1	500 (720), 380 (7000), 270 (49000)	620	7%	140
2	500 (670), 380 (6700), 270 (46000)	630	3%	145

[a] ε = molar absorption coefficient. [b] Quantum yield ϕ_{PL} measured in degassed solution. In air saturated solution ϕ_{PL} is slightly smaller and amounts to 6% for **1** and about 2.5% for **2**. [c] Decay time τ measured in degassed solution. In air saturated solution τ decreases to 115 ns for **1** and 110 ns for **2**, respectively.

$\lambda_{abs} > 360$ nm. In particular, both complexes show very weak absorption bands ($\varepsilon_{max} \approx 700\ M^{-1}cm^{-1}$; Table 1) centered at 500 nm. In analogy to similar iridium complexes,[13–15] the strong, high energy bands are assigned to $\pi \rightarrow \pi^*$ transitions within the ptpy and terpy ligands. The weak, lower energy bands are assigned to various charge transfer transitions involving metal and ligands. The spectra of **1** and **2** essentially resemble the spectrum of the parent complex $[Ir(ppy)_2(\kappa^2N\text{-terpy})][PF_6]$, with ppy = 2-phenylpyridinato and terpy = 2,2′-terpyridine,[15] with the exception of the weak band at 500 nm which had not been resolved.[15] Interestingly, the lowest band ($S_1 \leftarrow S_0$ transition) in **1** and **2** is separated from the next band by more than 0.5 eV in energy, as suggested by both the spectra and quantum chemical computations (see Supporting Information, Table S1). In related compounds with terpy replaced by a smaller diimine ligand, such as phenanthroline,[16,17] the lowest transition occurs at higher energy and overlaps spectrally with other charge transfer bands. Both complexes **1** and **2** are luminescent, showing broad unstructured emission spectra in the red spectral region. Ambient temperature spectra recorded in dichloromethane are centered at 620 nm (**1**) and 630 nm (**2**), respectively (see Figure 3). These emissions are red shifted compared to $[Ir(ppy)_2(\kappa^2N\text{-terpy})][PF_6]$ with unsubstituted terpy ligand, with the emission maximum at 590 nm,[15] by 0.1 eV and 0.13 eV, respectively. These red shifts are associated with lower π^* energies of PhCl-terpy and Cl-terpy due to enlargement of the aromatic system and electron withdrawing character of Cl, respectively.

Molecular and electronic structures of cations in **1** and **2** were calculated using stationary and time-dependent density functional theory (DFT and TD-DFT) methods. Pertinent results comprising the energies and character of photophysically relevant excited states are summarized in Table S1 in the

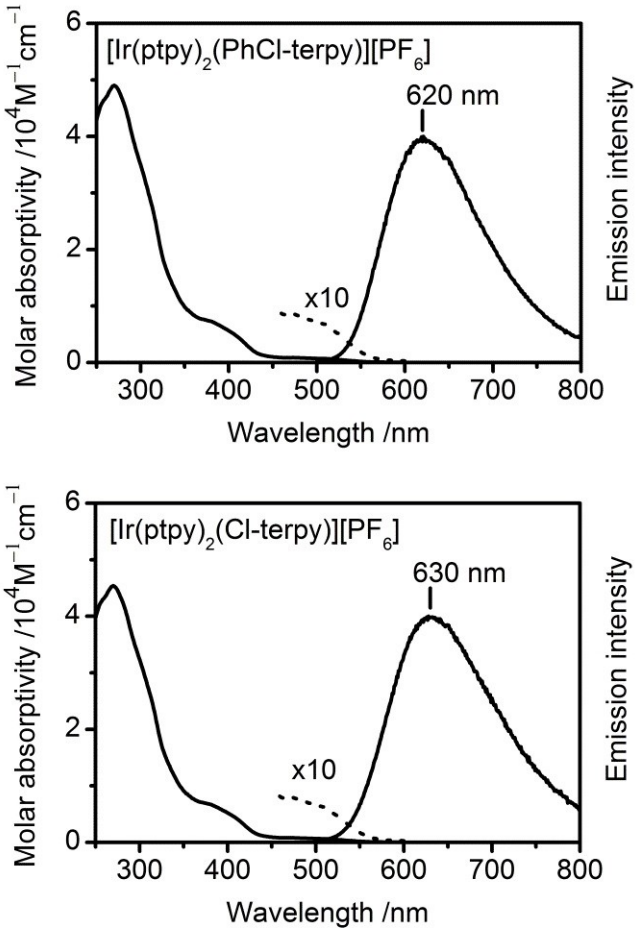

Figure 3. UV-Vis absorption and luminescence spectra of **1** and **2** in dichloromethane at ambient temperature. The low energy region of the absorption spectra in the range 450–600 nm was scaled up ten times for clarity.

Supplementary Information. For both complexes, the computations on ground state optimized geometry predict the lowest triplet state of significant mixed ligand-to-ligand charge transfer (LLCT) and metal-to-ligand charge transfer (MLCT) character, involving electron density shift from electron-rich ptpy ligands and Ir to electron-deficient terpy ligands (PhCl-terpy and Cl-terpy) in **1** and **2**, respectively. The calculated vertical energies are 2.033 eV for **1** and 1.983 eV for **2**. Thus, the emission of **2** is predicted to occur at slightly lower energy (longer wavelength) than that of complex **1**, reproducing the trend observed experimentally.

Biological Activity of 1 and 2

Along with photophysical properties of **1** and **2**, biological activities of these new compounds were investigated as well. To determine the cytotoxicity of both compounds, an MTT assay against two prominent human cancer cells, MCF-7 (breast adenocarcinoma) and HT-29 (colorectal adenocarcinoma), were conducted. Each assay was performed along with cisplatin (positive control). An overview of the determined IC_{50} values is shown in Table 2.

The complexes **1** and **2** show a significant increase in cytotoxicity in comparison to cisplatin in both tested cell lines. In the case of MCF-7, complex **1** and **2** show a nearly 20-fold increase in activity with an IC_{50} value of 2.1 μM and 1.8 μM, respectively. The IC_{50} value of cisplatin against MCF-7 ranged around 40 μM. It can be assumed, the additional phenyl group of **1** does not have a significant impact regarding cytotoxicity against MCF-7. In the case of HT-29 compound **1** and **2**, with an IC_{50} value of 2.0 μM and 3.2 μM, respectively, show an even higher increase of cytotoxicity. A nearly 48-fold increase for **1** and 30-fold for **2**. The IC_{50} value of cisplatin against HT-29 cancer cells ranged around ~95 μM due to higher cisplatin resistance and thus less efficiency against slow growing colon cancer cells.[18,19] The structural difference between **1** and **2** does not show any notable effect on the cytotoxicity against HT-29 as well. The immense increase in biological activity could be explained by the choice of the ligands. Iridium complexes with bipyridine ligands have excellent photophysical properties, and those were exploited for the switch-on detection of G-quadruplexes,[20] and as photosensitizers.[21] It has been suggested that simple $[Ir(ppy)_2(bpy)]^+$ complexes (ppy – phenylpyridinato) localize in membranes and induce ER stress and mitochondria-mediated apoptosis.[22] In the present case, the complex itself is of similar geometry with three bidentate ligands in an octahedral geometry. However, with an additional pending pyridine moiety and further substituents it may be necessary to re-examine the mechanism of action of the complexes as potential anti-cancer drugs to fully understand the differential activity of these metal complexes towards human cancer as well as healthy cells.

Table 2. Final IC_{50} values in μM (determined by MTT assay) for **1** and **2** against MCF-7 and HT-29 cells. All data were measured in triplicates and 48 h incubation time, in overall three independent experiments. Each assay was performed with cisplatin as positive control and untreated cells as negative control (only 0.5% DMSO). The experimental conditions were identical in each experiment, with a final concentration of 0.5% DMSO in all cases.

	IC_{50}[μM] MCF-7	IC_{50} [μM] HT-29
1	2.07 ± 0.05	2.00 ± 0.25
2	1.84 ± 0.17	3.22 ± 0.72
cisplatin	39.4 ± 5.7	96.3 ± 7.9

Conclusions

The synthesis and characterization of two new bis-cyclometalated compounds of the type $[Ir(ptpy)_2(N\hat{}N)]PF_6$ [N^N = κ^2*N*-terpy-C_6H_4Cl-*p* = 4'-(4-chlorophenyl)-2,2':6',2''-terpyridine, (**1**), and $[Ir(ptpy)_2(\kappa^2N$-terpy-Cl$)]PF_6$ (terpy-Cl = 4'-chloro-2,2':6',2''-terpyridine, (**2**)] was described. The characterization includes the confirmation of the molecular structure of **1** and **2** in the solid state by X-ray single crystal structure determination. The complexes **1** and **2** are luminescent at ambient temperature and exhibit broad unstructured luminescence in the red spectral region with the emission maxima in dichloromethane around 630 nm. Moreover, the biological activity of compounds **1** and **2** was investigated by MTT assays. Both species exhibit considerable cytotoxic effects towards two cancer cell lines (HT29 and MCF-7) showing significant IC_{50} values in the low micromolar range around 2–3 μM, significantly better than those of cisplatin in all cases. Further biological studies are necessary to understand the mechanism of action in detail and possibly improve the anti-cancer properties of compounds **1** and **2**.

Experimental Section

General: All manipulations were performed under an atmosphere of dry nitrogen using conventional Schlenk techniques. Solvents were dried with standard procedures and stored under nitrogen. 2-(*p*-tolyl)pyridine and the substituted terpyridines were purchased from Sigma-Aldrich and used as received. The starting complex $[\{Ir(\mu\text{-Cl})(ptpy)_2\}_2]$ was prepared following our literature method.[23] NMR spectra were recorded using a Jeol Eclipse 400 instrument. Chemical shifts were referenced to the CD_2Cl_2 signal δ = 5.31 ppm for ^1H and 53.8 ppm for $^{13}C\{^1H\}$ NMR spectra. Mass spectra were obtained with a JeolMstation JMS 700 instrument. Elemental analyses (C, H, N) were performed by the Microanalytical Laboratory of the Department of Chemistry, LMU Munich, using a Heraeus Elementar Vario EL instrument.

Photophysical measurements

UV/vis absorption spectra were measured using a Varian Cary 300 double-beam spectrometer with the sample held in a quartz cuvette of path length 1 cm. Emission spectra were measured with a Jobin Yvon Fluorolog-3 steady-state fluorescence spectrometer. Photoluminescence quantum yields were determined with a Hamamatsu C9920-02 system. The emission decay times were measured using a PicoBright PB-375 pulsed diode laser (λ_{exc} = 378 nm, pulse width 100 ps) as an excitation source. The PL signal

was detected with a cooled photomultiplier attached to a FAST ComTec multichannel scalar PCI card with a time resolution of 250 ps.

TD-DFT computations

Quantum mechanical computations were carried out using the NWChem. 6.6 computer program package.[24] The molecular structures were optimized using the B3LYP functional and Def2-SVP atomic basis set for all atoms except Ir, for which Def2-TZVP basis set with appropriate effective core potentials was used.[25] For these ground state geometries, 8 singlet and triplet excitations were calculated using the same functional and atomic basis sets, respectively.

Biological activities

Dulbecco's Modified Eagle's Medium (DMEM), containing 10% fetal calf serum, 1% penicillin and streptomycin, was used as growth medium. MCF-7 and HT-29 cells were detached from the wells with trypsin and EDTA, harvested by centrifugation and resuspended again in the cell culture medium. The assays were carried out on 96 well plates with 6000 cells per well for MCF-7 and HT-29. After 24 h of incubation at 37 °C and 10% CO_2, the cells were treated with compounds **1** and **2** (constant DMSO concentrations of 0.5%) with a final volume of 200 µl per well. For a negative control, one series of cells were only treated by 0.5% DMSO. The cells were incubated for 48 h followed by adding 50 µl MTT (2.5 mg/ml). After an incubation time of 2 h, the medium was removed and 200 µl DMSO were added. The formazan crystals were dissolved, and the absorption was measured at 550 nm, using a reference wavelength of 620 nm. Each test was repeated in triplicates in three independent experiments for each cell line, along with cisplatin as the positive control.

Synthesis of 1 and 2: To a solution of $[\{Ir(\mu\text{-}Cl)(ptpy)_2\}_2]$ (0.15 mmol) in 25 mL of a mixture of CH_2Cl_2/MeOH/H_2O (1 : 1 : 0.5) the terpy-R ligand (0.3 mmol) was added and the mixture refluxed with stirring for 2 h. After cooling to room temperature, KPF_6 (0.50 mmol) was added and the solution stirred for additional 20 minutes. The solvent was removed to dryness in vacuo and the residue dissolved in dichloromethane and chromatographed on alumina with CH_2Cl_2 as the eluent. The resulting solution was evaporated to dryness and the residue was re-dissolved in 5 ml of dichloromethane and the product precipitated by diethyl ether.

$[Ir(ptpy)_2(\kappa^2N\text{-terpy-}C_6H_4\text{-Cl-}p)]PF_6$ (1) Yield: 140 mg (91%). *Anal.* $C_{45}H_{34}ClF_6IrN_5P$ (1017.43): C, 53.12; H, 3.37; N, 6.88. Found: C, 53.33; H, 3.54; N, 6.55%. **MS** (FAB^+): $m/z = 872.21$ [M^+] complex cation. **^1H NMR** (400 MHz, CD_2Cl_2): δ = 8.99 (d, J = 5.6 Hz, 1H), 8.66 (d, J = 2.0 Hz, 1H), 8.65 (s, 1H), 8.23 (d, J = 4.4 Hz, 1H), 8.15 (dt, J = 1.6 Hz, J = 8.0 Hz, 1H), 7.76 (m, 8H), 7.54 (m, 4H), 7.36 (m, 2H), 7.23 (d, J = 9.6 Hz, 1H), 7.09 (m, 2H), 6.93 (m, 2H), 6.81 (d, J = 11.2 Hz, 1H), 6.53 (d, J = 8.0 Hz, 1H), 6.46 (dd, J = 8.0 Hz, J = 1.6 Hz, 1H), 5.73 (s, 1H), 2.00 (s, 3H), 1.84 (s, 3H). **$^{13}C\{^1H\}$ NMR** (100 MHz, CD_2Cl_2): δ = 168.2, 166.6, 163.4, 157.8, 156.7, 156.0, 152.4, 150.4, 150.2, 147.8, 147.7, 146.7, 140.9, 140.5, 139.8, 139.4, 139.3, 138.0, 137.9, 137.3, 135.7, 133.7, 133.1, 131.3, 129.8, 129.6, 128.8, 127.8, 126.0, 125.4, 124.6, 123.8, 123.7, 123.4, 122.5, 122.4, 122.2, 122.1, 121.2, 119.0, 118.9, 21.6, 21.5.

$[Ir(ptpy)_2(\kappa^2N\text{-terpy-Cl})]PF_6$ (2) Yield: 135 mg (92%). *Anal.* Calc. for $C_{39}H_{30}ClF_6IrN_5P$ (941.34): C, 48.76; H, 3.21; N, 7.44. Found: C, 48.92; H, 3.51; N, 7.19%. **MS** (FAB^+): $m/z = 796.18$ [M^+] complex cation. **^1H NMR** (400 MHz, CD_2Cl_2): δ = 8.97 (d, J = 5.6 Hz, 1H), 8.26 (d, J = 4.4 Hz, 1H), 8.15 (dt, J = 8.0 Hz, J = 1.6 Hz, 1H), 7.78 (m, 5H), 7.50 (d, J = 8.0 Hz, 1H), 7.41 (m, 1H), 7.39 (d, J = 1.6 Hz, 1H), 7.27 (d, J = 5.6 Hz, 2H), 7.24 (d, J = 8.0 Hz, 2H), 7.09 (m, 2H), 6.95 (m, 2H), 6.79 (d, J = 6.8 Hz, 1H), 6.49 (d, J = 7.6 Hz, 1H), 6.45 (dd, J = 8.0 Hz, J = 1.6 Hz, 1H), 5.64 (s, 1H), 5.11 (s, 1H), 1.99 (s, 3H), 1.86 (s, 3H). **$^{13}C\{^1H\}$ NMR** (100 MHz, CD_2Cl_2): δ = 168.2, 166.4, 163.8, 158.5, 155.6, 154.9, 152.4, 150.6, 149.6, 148.0, 147.7, 147.5, 145.7, 141.0, 140.3, 139.7, 139.5, 139.4, 138.2, 138.0, 135.9, 133.2, 131.2, 128.8, 128.3, 125.4, 124.6, 124.0, 123.9, 123.8, 123.7, 122.5, 122.4, 122.3, 122.2, 119.1, 119.0, 21.6, 21.4.

X-ray Structural Determination: Crystals of **1** and **2** suitable for X-ray diffraction were obtained by crystallization from mixtures of dichloromethane/methanol/*iso*-hexane at ambient temperature. Crystals were selected by means of a polarization microscope, mounted on a MiTeGen MicroLoop, and investigated with a Bruker D8 Venture TXS diffractometer using Mo-Kα radiation (λ = 0.71073 Å). The structures were solved by direct methods (SHELXT)[26] and refined by full-matrix least-squares calculations on F^2 (SHELXL-2014/7).[27] In **1**, the disorder of CH_2Cl_2 has been described by a split model with isotropic refinement of all disordered atoms. The ratio of site occupation factors of the two disordered parts was refined to 0.56/0.44. All C–Cl distances of CH_2Cl_2 have been restrained to be equal within a standard deviation of 0.01 Å, all Cl–Cl distances have been refined to be equal within a standard deviation of 0.02 Å. In **2**, the disorder of PF_6^- has been described by a split model with the non-disordered PF_6^- acting as geometrical model for the disordered one. All disordered atoms have been refined isotropically. Solvent electron densities that could not be modelled properly have been squeezed-out.[28] According to Platon Squeeze there is one big void with a volume of 383 Å^3 and 105 squeezed-out electrons. This fits for two CH_2Cl_2 and one CH_3OH. Details of the crystal data, data collection, structure solution, and refinement parameters of compound **1** and **2** are summarized in Table 3. Crystallographic data (excluding structure factors) for the structures in this paper have been deposited with the Cambridge Crystallographic Data Centre, CCDC, 12 Union Road, Cambridge CB21EZ, UK. Copies of the data can be obtained free of charge upon quoting the depository

Table 3. Experimental details of the crystal structure determination of **1** and **2**.

Compound	**1**	**2**
Empirical formula	$C_{46}H_{36}F_6Cl_3IrN_3P$	$C_{39}H_{30}F_6ClIrN_5P$
Formula weight	1102.32	941.30
Temperature/K	173 (2)	173 (2)
Crystal system	monoclinic	triclinic
Space group	$P2_1/n$	$P\bar{1}$
a/Å	13.6545(12)	14.8418(17)
b/Å	14.8842(12)	16.5923(19)
c/Å	21.9597(18)	17.128(2)
α/°	90	92.967(4)
β/°	106.814(3)	112.989(4)
γ/°	90	99.725(4)
Volume/Å^3	4272.2(6)	3794.8(8)
Z	4	4
ρ calcd./g·cm^{-3}	1.714	1.648
μ /mm^{-1}	3.418	3.696
θ range/°	2.737–27.485	2.861–29.131
Reflections, collected	89501	94912
Reflections, independent	9794	20386
R_{int}	0.0771	0.0460
wR_2 (all data)	0.0708	0.0792
R_1	0.03	0.0296
S	1.039	1.041
$\Delta\rho_{fin}$ (max/min)/e·Å^{-3}	0.788/−1.061	1.403/−1.297

number CCDC-2130005 (**1**) and CCDC-2130004 (**2**) (Fax: +44-1223-336-033; E-Mail: deposit@ccdc.cam.ac.uk, http://www.ccdc.cam.ac.uk).

Acknowledgements

The authors are grateful to the Department of Chemistry of the Ludwig-Maximilians-Universität Munich for financial support. Open access funding enabled and organized by Projekt DEAL. Open Access funding enabled and organized by Projekt DEAL.

Conflict of Interest

The authors declare no conflict of interest.

Data Availability Statement

The data that support the findings of this study are available in the supplementary material of this article.

Keywords: Cyclometalated complexes · Cytotoxic activity · Iridium · Organometallic anticancer drugs · Terpyridine ligands

[1] a) K. J. Franz, N. Metzler-Nolte, *Chem. Rev.* **2019**, *119*, 727; b) C. G. Hartinger, N. Metzler-Nolte, P. J. Dyson, *Organometallics* **2012**, *31*, 5677; c) G. Gasser, N. Metzler-Nolte, *Curr. Opin. Chem. Biol.* **2012**, *16*, 84; d) N. Metzler-Nolte, in: *Medicinal Organometallic Chemistry, Vol. 32* (Eds.: G. Jaouen, N. Metzler-Nolte), Springer, Heidelberg, **2010**, pp. 195–217; e) G. Gasser, I. Ott, N. Metzler-Nolte, *J. Med. Chem.* **2011**, *54*, 3.
[2] a) A. Zamora, G. Vigueras, V. Rodríguez, M. D. Santana, J. Ruiz, *Coord. Chem. Rev.* **2018**, *360*, 34; b) L. He, K.-N. Wang, Y. Zheng, J.-J. Cao, M.-F. Zhang, C.-P. Tan, L.-N. Ji, Z.-W. Mao, *Dalton Trans.* **2018**, *47*, 6942.
[3] P. Laha, U. De, F. Chandra, N. Dehury, S. Khullar, H. S. Kim, S. Patra, *Dalton Trans.* **2018**, *47*, 15873.
[4] a) L.-J. Liu, W. Wang, S.-Y. Huang, Y. Hong, G. Li, S. Lin, J. Tian, Z. Cai, H.-M. D. Wang, D.-L. Ma, C.-H. Leung, *Chem. Sci.* **2017**, *8*, 4756; b) H.-J. Zong, L. Lu, K. H. Leung, C. C. L. Wong, C. Peng, S.-C. Yan, D.-L. Ma, Z. Cai, H.-M. D. Wang, C.-H. Leung, *Chem. Sci.* **2015**, *6*, 5400.
[5] R. Cao, J. Jia, X. Ma, M. Zhou, H. Fei, *J. Med. Chem.* **2013**, *56*, 3636.
[6] J.-J. Cao, C.-P. Tan, M.-H. Chen, N. Wu, D.-Y. Yao, X.-G. Liu, L.-N. Ji, Z.-W. Mao, *Chem. Sci.* **2017**, *8*, 631.
[7] I. Gamba, I. Salvado, R. F. Brissos, P. Gamez, J. Brea, M. I. Loza, M. E. Vazquez, M. V. Lopez, *Chem. Commun.* **2016**, *52*, 1234.
[8] V. Novohradsky, A. Zamora, A. Gandioso, V. Brabec, J. Ruiz, V. Marchán, *Chem. Commun.* **2017**, *53*, 5523.
[9] a) N. Lu, Y. Luo, Q. Zhang, P. Zhang, *Dalton Trans.* **2020**, *49*, 9182; b) L. C.-C. Lee, A. W.-Y. Tsang, H.-W. Liu, K. K.-W. Lo, *Inorg. Chem.* **2020**, *59*, 14796.
[10] P. Yang, S. Zhang, K. Wang, H. Qi, *Dalton Trans.* **2021**, *50*, 17338 and references cited therein.
[11] M. Graf, H.-C. Böttcher, N. Metzler-Nolte, K. Sünkel, S. Thavalingam, R. Czerwieniec, *Z. Anorg. Allg. Chem.* **2021**, *647*, 519 and references cited therein.
[12] D. P. Ris, G. E. Schneider, C. D. Ertl, E. Kohler, T. Müntener, M. Neuburger, E. C. Constable, C. E. Housecroft, *J. Organomet. Chem.* **2016**, *812*, 272.
[13] J. C. Deaton, F. N. Castellano, *Archetypal Iridium(III) Compounds for Optoelectronic and Photonic Applications, in: Iridium(III) in Optoelectronic and Photonic Applications* (Ed.: E. Zysman-Colman) 2017, Wiley-VCH, Weinheim, pp 1–69.
[14] H. Yersin, A. F. Rausch, R. Czerwieniec, T. Hofbeck, T. Fischer, *Coord. Chem. Rev.* **2011**, *255*, 2622.
[15] E. C. Constable, C. E. Housecroft, G. E. Schneider, J. A. Zampese, H. J. Bolink, A. Pertegás, C. Roldan-Carmona, *Dalton Trans.* **2014**, *43*, 4653.
[16] H. J. Bolink, L. Cappelli, S. Cheylan, E. Coronado, R. D. Costa, N. Lardiés, K. Nazeeruddin, E. Ortí, *J. Mater. Chem.* **2007**, *17*, 5032.
[17] M. Graf, R. Czerwieniec, P. Mayer, H.-C. Böttcher, *Inorg. Chim. Acta* **2021**, 527, 120554.
[18] K. J. Scanlon, M. Kashani-Sabet, T. Tone, T. Funato, *Pharmacol. Ther.* **1991**, *52*, 385.
[19] A. Stockert, D. Kinder, M. Christ, K. Amend, A. Aulthouse, *Austin J. Pharmacol. Ther.* **2014**, *2*, 6.
[20] a) S. Lin, W. Gao, Z. R. Tian, C. Yang, L. H. Lu, J. L. Mergny, C. H. Leung, D. L. Ma, *Chem. Sci.* **2015**, *6*, 4284; b) S. Lin, B. He, C. Yang, C.-H. Leung, J.-L. Mergny, D.-L. Ma, *Chem. Commun.* **2015**, *51*, 16033.
[21] C. Mari, H. Y. Huang, R. Rubbiani, M. Schulze, F. Würthner, H. Chao, G. Gasser, *Eur. J. Inorg. Chem.* **2017**, 1745.
[22] R. Cao, J. Jia, X. Ma, M. Zhou, H. Fei, *J. Med. Chem.* **2013**, *56*, 3636.
[23] H.-C. Böttcher, M. Graf, K. Sünkel, P. Mayer, H. Krüger, *Inorg. Chim. Acta* **2011**, *365*, 103.
[24] M. Valiev, E. J. Bylaska, N. Govind, K. Kowalski, T. P. Straatsma, H. J. J. van Dam, D. Wang, J. Nieplocha, E. Apra, T. L. Windus, W. A. de Jong, *Comput. Phys. Commun.* **2010**, *181*, 1477.
[25] B. P. Pritcahard, D. Altarawy, B. Didier, T. D. Gibson, T. L. Windus, *J. Chem. Inf. Model.* **2019**, 59, 4814.
[26] G. M. Sheldrick, *Acta Crystallogr.* **2015**, *A71*, 3.
[27] G. M. Sheldrick, *Acta Crystallogr.* **2015**, *C71*, 3.
[28] A. L. Spek, *Acta Crystallogr.* **2015**, *C71*, 9.

Manuscript received: February 2, 2022
Revised manuscript received: March 26, 2022

